doi:10.20944/preprints202101.0112.v1

Future changes in precipitation extremes over East Africa based on CMIP6 projections

Brian Ayugi[1,2]*, Victor Dike[3,4], Hamida Ngoma[2], Hassen Babaousmail[5], Victor Ongoma[6]

[1]Jiangsu Key Laboratory of Atmospheric Environment Monitoring and Pollution Control, Collaborative Innovation Center of Atmospheric Environment and Equipment Technology, School of Environmental Science and Engineering, Nanjing University of Information Science and Technology, Nanjing 210044, China

[2]Key Laboratory of Meteorological Disaster, Ministry of Education (KLME)/Joint International Research Laboratory of Climate and Environment Change (ILCEC)/Collaborative Innovation Center on Forecast and Evaluation of Meteorological Disasters (CIC-FEMD), Nanjing, University of Information Science and Technology, Nanjing 210044, China

[3]International Center for Climate and Environment Sciences, Institute of Atmospheric Physics, Chinese Academy of Sciences, Beijing 100029, China

[4]Energy, Climate, and Environment Science Group, Imo State Polytechnic Umuagwo, Ohaji, PMB 1472 Owerri, Imo State, Nigeria

[5]Binjiang College of Nanjing University of Information Science and Technology, Jiangsu, Wuxi, China

[6]International Water Research Institute, Mohammed VI Polytechnic University, Lot 660, Hay Moulay Rachid, Ben Guerir, 43150, Morocco

*Corresponding author: ayugi.o@gmail.com; bayugi@nuist.edu.cn

Abstract

This paper presents an analysis of precipitation extremes over the East African region. The study employs six extreme precipitation indices defined by the Expert Team on Climate Change Detection and Indices (ETCCDI) to evaluate possible climate change. Observed datasets and CMIP6 simulations and projections are employed to assess the changes during the two main rainfall seasons of March to May (MAM) and October to December (OND). The study evaluated the capability of CMIP6 simulations in reproducing the observed extreme events during the period 1995 – 2014. Our results show that the multi-model ensemble (herein referred to as MME) of CMIP6 models can depict the observed spatial distribution of precipitation extremes for both seasons, albeit with some noticeable exceptions in some indices. Overall, MME's assessment yields considerable confidence in CMIP6 to be employed for the projection of extreme events over the study area. Analysis of extreme estimations shows an increase (decrease) in CDD (CWD) during 2081 – 2100 relative to the baseline period in both seasons. Moreover, SDII, R95p, R20mm, and PRCPTOT demonstrate significant OND estimates compared to the MAM season. The spatial variation for extreme incidences shows likely intensification over Uganda and most parts of Kenya, while reduction is observed over the Tanzania region. The increase in projected extremes during two main rainfall seasons poses a significant threat to the sustainability of societal infrastructure and ecosystem wellbeing. The results from these analyses present an opportunity to understand the emergence of extreme events and the capability of model outputs from CMIP6 in estimating the projected changes. More studies are encouraged to examine the underlying physical features modulating the occurrence of extremes incidences projected for relevant policies.

Keywords: CMIP6, extreme precipitation, model evaluation, east Africa

1. Introduction

The frequent occurrence of extreme events such as heatwaves, droughts, pluvial events, and hurricanes over the recent years points to clear evidence of global warming (GW) and climate change (Alexander et al., 2006; Sillmann et al., 2013; IPCC, 2014; Alexander, 2016). The recent IPCC special report on impacts of global warming of 1.5 ºC estimate that GW is likely to attain 1.5 ºC by 2030 and 2052 if the global community maintain "business as usual" scenario (IPCC, 2018). The resultant response of climate systems will depict features associated with increased intensity of precipitation extremes, a sharp decline in the number of wet spell lengths, and an increase in dry spell lengths (Giorgi et al., 2019). The unprecedented impacts of climate extremes threaten human health, economic stability, and stability of natural and build infrastructure (AghaKouchak et al., 2020). Thus, characterizing the response of the anthropogenic climate change, which results in extreme events such as an increase both the intensity and frequency at the regional or local level is an imperative task. This will aid decision and policymakers and planners in developing future adaptation strategies.

Global and regional changes have been noted with substantial upsurge detected over Europe (Fischer and Knutti, 2016; Paplexious and Monanari, 2019), China (Jiang et al., 2012; Yuan et al., 2015; Chen and Sun, 2018; Zhu et al., 2020) and US (Paplexious and Monanari, 2019; Janssen et al., 2014; Kukel et al., 2008; Akinsanola et al., 2020), among other regions. Consequently, much progress has been made to enhance our understanding of the recent changes and possible attributions that links extreme events to the global warming even though the full scientific is deficient (Fischer and Knutti, 2016; Sillman et al., 2013; Myhre et al., 2017;

Kunkel et al., 2008; Pendegrass, 2018). Overall, an increase in moisture as a result of shifts in the dynamical processes has been noted to drive amplification of precipitation intensity.

Comparable to other regions, Africa stands out as one of the most susceptible areas to climate variability and change (Niang et al., 2014). Numerous studies agree that the region above is experiencing an observed change in climate patterns (Trenberth, 2011; Anguilar et al., 2009; Shongwe et al., 2011; Omondi et al., 2014; Taylor et al., 2017). For instance, many subregions have experience notable changes in precipitation frequency, intensity, and quantity of occurrence over the recent decades (Trenberth, 2011; Donat et al., 2013; Alexander, 2016). Similarly, positive trajectories in temperature have been observed and projected to increase significantly (Collins, 2011; Senevirante, 2012; Niang et al., 2014; Ongoma et al., 2018a). This will affect the broader population's livelihoods that rely entirely on rainfed agriculture to support the economy (FAO, 2019). Further, the projected increase in temperature will intensify moisture loss through amplified evapotranspiration and strengthen the occurrence of drought hazards (Funk et al., 2012; Van Loon, 2019; Ayugi et al., 2020a; Tan et al., 2020).

Despite the widespread evidence of extreme events occurrences, regional variation is noted due to complex physiographical features and processes, resulting in varying responses to the global-scale change (IPCC, 2013). Using the global climate models outputs derived from Coupled Intercomparison Project Phase five (CMIP5; Taylor, 2012), varying researchers have reported this phenomenal of regional variability in the extent, duration, frequency, and intensity of extreme climate events (Zhang et al., 2011; Jiang et al., 2012, 2015; Fischer et al., 2015). A recent study (Weber et al., 2018) observed that temperature projections in sub-Saharan Africa (SSA) is to be higher than the global mean temperature increase. To illustrate, the region situated between 15ºS and 15ºN is projected to experience an amplification in hot nights, coupled with much longer and more frequent heatwaves (Kharin et al., 2018). Thus, it is paramount to characterize the regional trends and future variations of extreme events for robust adaptation and risk management strategies.

East Africa (EA) witnesses' unusual occurrences of signature immoderate events such as droughts and floods (Viste et al., 2013; Liebmann et al., 2014; Kilavi et al., 2018; Ayugi et al., 2020a; Ongoma et al., 2018a, b). The region located in the tropics and bound along latitude 12ºS - 5ºN and longitude 28º E - 42ºE will need humanitarian assistance if no proper mechanism is put in place. Several studies based mainly on CMIP5 or regional climate models (RCMs) have been conducted to examine to historical trends and future projections of extremes events of the EA region (Ongoma et al., 2018c; Gebrechorkos et al., 2018; Osima et al., 2018; Onyutha, 2020; Ogega et al., 2020; Tegegne et al., 2020). Undoubtedly, these studies' overall conclusion shows a varying trend of change, mainly attributed to the data sets employed or period analysed.

Essentially, temperature extremes (i.e., minimum and maximum temperature) show an overall upward tendency in many studies (IPCC, 2014; Ongoma et al., 2018a; Gebrechorkos et al., 2018; Osima et al., 2018). Conversely, projections in precipitation extremes using indices developed by the Expert Team on Climate Change Detection and Indices (ETCCDI; Klein Tank et al., 2009; Zhang et al., 2011) are marred by uncertainty and unclear patterns (Osima et al., 2018; Ogega et al., 2020; Onyutha, 2020). To demonstrate, Onyutha (2020) showed significant biases in RCMs employed in simulating maximum wet spell (MWS) over the EA region. Similar uncertainty in precipitation projections is noted across the Greater Horn of Africa (GHA), in a study that utilized a large 25-member RCMs and employed robust technique for detecting climate change signal (Osima et al., 2018). There remains an urgent need for reliable projections of precipitation extremes over the EA region for appropriate measures to be put in place to cushion the population from the adverse impacts of unforeseeable impacts.

The new generation model outputs of phase six (CMIP6; Eyring et al., 2016) provide an opportunity to improve our understanding of climate change impacts resulting from exacerbated global warming. Policymakers and community workers are in dire need of timely information that will enable them to address pertinent issues such as those that pinpoint exact tendencies of historical changes, the magnitude of the shift, and future projections. Presently, no studies to our understanding have attempted to use the models' outputs from CMIP6 with improved parameterization schemes and higher spatial-temporal resolution (e.g., from ~0.7° to ~2.8°) in assessing the projected changes in precipitation extremes over the EA region. Moreover, the new pathways representing a range of future greenhouse gas emissions and land-use change scenarios promise a robust estimate of future projections of hydroclimate variables. They incorporate various assumptions about socio-economic growth, climate mitigation efforts, and global governance (O'Neill et al., 2016).

Consequently, the present study seeks to add to the concerted efforts being undertaken to enhance our understanding of extreme precipitation events' potential occurrence. In particular, the study assesses CMIP6 models' performance in simulating precipitation extremes over the EA domain and further examines the projected changes of EA's extremes under Shared Socio-economic Pathways (SSP2 – 4.5 and SSP5 – 8.5). This will enable decisions and policymakers to develop robust policies for sustainable development. The rest of the paper is structured as follows: section 2 elaborates more on the data and methods used, while section 3 gives the analyses' results. Lastly, discussion and conclusion are presented in section 4

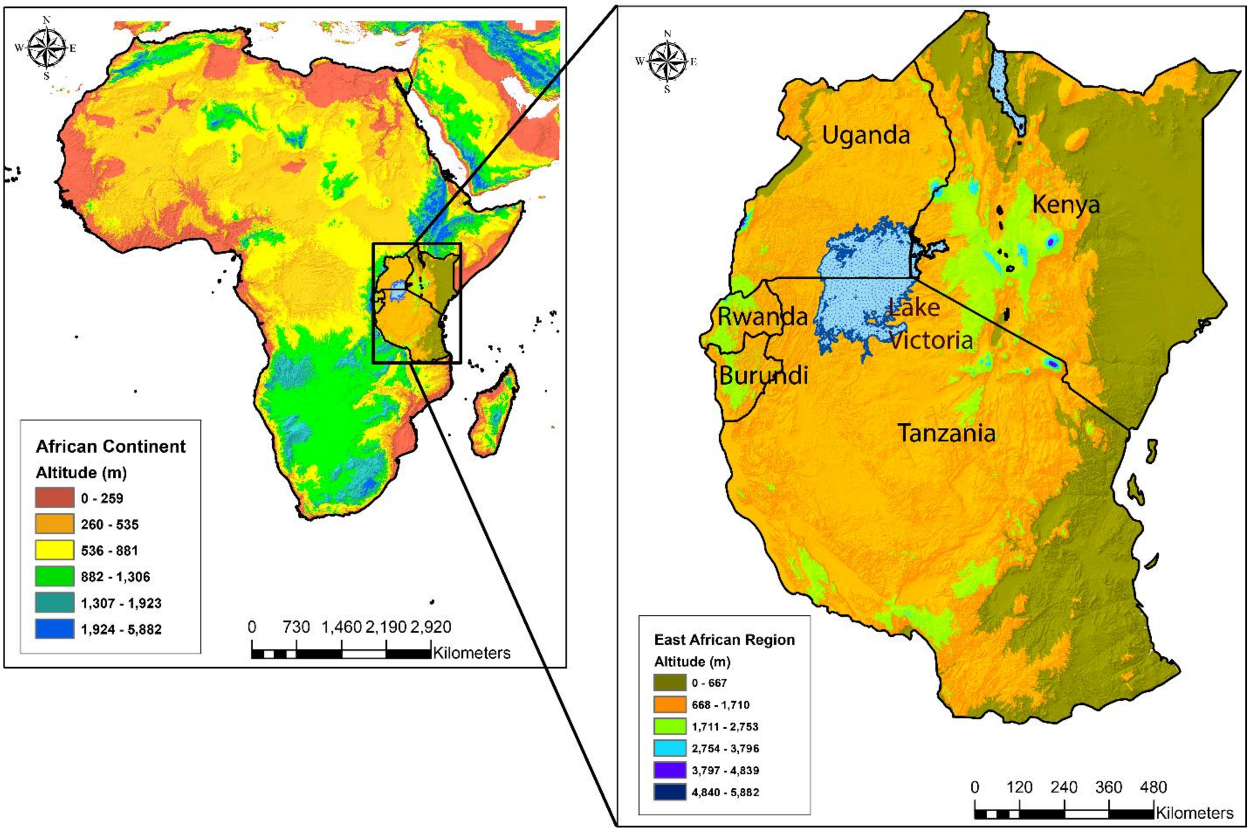

Figure 1. The map of Africa delineating different sub-regions. The east Africa region marked as with countries considered for analysis in this study.

2. Data Methods

2.1 Data

The study utilized CMIP6 model outputs from DECK experiment (Eyring et al., 2016) accessed through Earth Systems Grid Federation data centers. The daily precipitation variable (*pr*) for historical experiment and two future SSP2-4.5 and SSP5-8.5 are used in the estimation of extreme precipitation events. The SSP-forcing denotes an integrated scenario of possible future climate and societal change, which would be employed to assess issues such as the mitigation and adaptation efforts needed to attain a particular climate outcome (O'Neill et al., 2016). The choice for the two scenarios from the available five possible framework was informed by the assumption that differences in climate outcomes produced by varying scenarios for the same global pathways are likely small relative to varying features of regional climate or/and inter-model uncertainties (O'Neill et al., 2016). The historical experiment starts from 1850 – 2014 while forcing datasets under Scenario Model Intercomparison Project (Scenario MIP; O'Neill et al., 2016) starts from 2015 – 2100. In this study, we selected a baseline period of 1995 – 2014 whereas two future period referred herein as near-future (2021 – 2040) and far-future

(2081 – 2100), respectively. This study utilized the first realization (r1i1p1f1) from fifteen models that have relatively higher spatial resolution (~ 1°). Due to the inherent uncertainties of individual GCMs, the mean ensemble average was employed for its robust estimates compared to each model. **Table 1** denotes the model description, including the spatial resolution, the institute(s) possessing the intellectual property rights, the abbreviate name, and key reference(s) for further detailed information.

For the observed datasets, the current work utilized satellite-derived datasets from Climate Hazards Group InfraRed with Station data version two (CHIRPSv2). The datasets are available on a global scale (i.e., 50°S - 50°N) and begin from 1981 to the present day on varying timescales. Developed by a lead scientist from the US Geological Survey, the CHIRPS data integrates satellite imagery with a native horizontal grid increment of approximately ~ 27.75 km. Funk et al. (2015) detailed more information regarding datasets. The dataset's suitability in reproducing observed climate over the study domain has been proven in previous studies (e.g., Gebrechorkos et al., 2017; Kimani et al., 2017; Ayugi et al., 2019). Because of different grid scales, all datasets were re-gridded to 1° x 1° using a remapping technique conducted in the Climate Data Operator toolkit (CDO). The analyses to examine changes in precipitation extremes was conducted for two seasons, namely, March to May (MAM) and for October to December (OND). The MAM season represent period when the region receives more rainfall and locally referred as 'long-rains' while OND show winter precipitation, also known as 'short-rains'. The regional climatology and influencing factors regulating the occurrence of mean and extreme events are well detailed in previous studies (Ongoma et al., 2017; Nicholson, 2017; Camberlin, 2018).

Table 1. Information of the fifteen CMIP6 climate models used in this study

S/N	Models	Institution	Resolution	Reference
1	BCC-CSM2-MR	Beijing Climate Center and China Meteorological Administration, China	1.13° ×1.13°	Wu et al. 2019
2	EC-EARTH3	EC-EARTH consortium, Sweden	0.70°×0.70°	(E-C Earth, 2019b)
3	EC-EARTH3-Veg	EC-EARTH consortium, Sweden	0.70°×0.70°	(E-C Earth, 2019a)
4	GFDL-ESM4	Geophysical Fluid Dynamics Laboratory (GFDL), USA	1.25°×1.00°	(John et al., 2018)
5	INM-CM4-8	Institute for Numerical Mathematics, Russian Academy of Science, Moscow, Russia	2.00°x1.50°	(Volodin et al., 2019)
6	INM-CM5-0	Institute for Numerical Mathematics, Russian Academy of Science, Moscow, Russia	2.00°x1.50°	(Volodin et al., 2019)
7	MPI-ESM1-2-HR	Max Planck Institute, Germany	0.90°×1.30°	(von Storch et al., 2017)

8	MRI-ESM2-0	Meteorological Research Institute (MRI), Japan	1.13º×1.13º	(Yukimoto et al., 2019)
9	NorESM2-MM	Climate modeling Consortium, Norway	0.90ºx1.25º	(Seland et al., 2020)
10	CESM	National Centre for Atmospheric Research (USA	0.94°×1.25°	Danabasoglu et al. (2019)
11	CESM-WACCM	National Centre for Atmospheric Research (USA	0.94°×1.25°	Danabasoglu et al. (2019)
12	FGOALS-G3	LASG, Institute of Atmospheric Physics, Chinese Academy of Sciences (China)	1.25° × 2.0°	Yongqiang et al (2018)
13	NESM3	Nanjing University of Information Science and Technology, China	1.125°× 1.125°	Cao et al (2019)
14	KACE-1-0-G	National Institute of Meteorological Sciences/Korea Meteorological Administration, Korea	1.25°× 1.875°	Byun et al, (2019)
15	CMCC-CM2-SR5	Fondazione Centro Euro-Mediterraneo sui Cambiamenti Climatici, Italy	1.0°× 1.0°	Fogli et al, (2020)

2.2 Methods

2.2.1 Model performance metric

As a first step, models were compared with observational data sets to examine their capability of simulating the observed mean and extreme events over the study area. The comparative analysis was conducted for the period 1995 – 2014, which corresponds to the modern baseline period for upcoming sixth assessment report. The statistical metrics of mean bias error (MBE), the root mean square distance (RMSD), and the pattern correlation (PC) was employed in this study to analyze the seasonal extreme simulation. For instance, the PC is used to check the relationship between the model and CHIRPS with -1 or 1 representing the range of perfect correlation or lack of similarity features in the two data sets. Similarly, the RMSD and MBE cross-examine the spread and accuracy of model data sets. The smaller values of the two metrics denote the best performance, while the more extensive distance denotes higher amplitudes than the observed values. Various studies, i.e., Wilks (2006), Chai and Draxler (2014), Ongoma et al. (2018c), and Ayugi et al. (2020b), highlights mathematical functions and necessary information regarding the approaches employed.

2.2.3 Climate extreme indices definition and calculation

This study used a suite of six precipitation extreme indices (Table 2) recommended by the ETCCDMI for monitoring and detection of climate change (Zhang et al, 2011). The listed indices mainly assess changes in the intensity, frequency, and duration of precipitation events over the study area. The indices can be divided into four main categories. Firstly, the duration

Preprints (www.preprints.org) | NOT PEER-REVIEWED | Posted: 6 January 2021 doi:10.20944/preprints202101.0112.v1

indices, which mainly defines periods of excessive wetness/dryness. Here we used consecutive dry days (CDD) and consecutive wet days (CWD). The CDD represents the length of the most prolonged dry spell in a year, while the CWD index represents the most extended wet spell in a year. Secondly, a percentile-based index that defines very wet days (R95P). The precipitation index used in this category represents the rainfall amount falling about the 95th (R95p). Thirdly, threshold-based indices, defined as the number of days in which precipitation value is above/below a fixed threshold. Here we defined the number of very heavy precipitation days > 20 mm (R20). Lastly, the study employed other indices that delineate the period of seasonal precipitation total (PRCPTOT) and those that defines precipitation intensity, such as the simple daily intensity index (SDII). The listed indices are intended to demonstrate the observed and projected change in extreme climate occurrences (Klein Tank et al., 2009; Zhang et al., 2011). More details regarding the indices are summarized in **Table 2**.

Table 2. Definitions and Units of Rainfall Indices Used in this study

ID	Name	Definitions	Units
PRCPTOT	Wet-day precipitation amount	Total precipitation in wet days (RR ≥ 1 mm), defined as PP_{ij} representing daily precipitation amount on day I in a period j. If the I denote the number of days in j, then; $PRCPTOT_j = \sum_{i=1}^{i} PP_{ij}$	mm
R95p	Extremely wet days	Total precipitation when PP > 95th percentile. Here, PP_{cd} be daily precipitation amount on a wet day *c* (PP≥1.0 mm) in a period *i* and *let* $PP_{cd^{95}}$. *where* 95^{th} percentile of precipitation on wet days in the baseline/projected period. If d represent the number of wet days in the period, then $R95P_j = \sum_{c=1}^{c} PP_{cd}$ *where* $PP_{cd} > PP_{cd^{95}}$	mm
SDII	Wet-day intensity	Average precipitation from wet-days. This can be defined as PP_{wj} be the daily precipitation amount on wet days, *w* (PP≥1 mm) in period j. If *w* represents number of wet days in j, then $SDII_j = \frac{\sum_{w=1}^{W} PP_{wj}}{W}$	mm/day
R20mm	Heavy precipitation days	Number of very heavy precipitation days (RR ≥ 20mm). That is; let PP_{ij} be the daily precipitation amount where $PP_{ij} \geq 20\ mm$	days
CDD	Consecutive dry days	Maximum number of consecutive dry days (RR ≤ 1 mm). Let PP_{ij} be the daily precipitation amount on day I in period j. Count the largest consecutive days where $PP_{ij} \leq 1mm$	days
CWD	Consecutive wet days	Maximum number of consecutive dry days (RR ≥ 1 mm). Let PP_{ij} be the daily precipitation amount on day I in period j. Count the largest consecutive days where $PP_{ij} \geq 1mm$	days

3.0 Results and Discussions

3.1 Evaluation of model performance

The first step of the analyses examined the capability of MME to simulate the observed mean and extreme events over the study area. The spatial distribution of the six extreme indices used (listed in table 2) are displayed in Figure 1 (MAM) and Figure 2 (OND). The study employed

CHIRPS as observation datasets to analyze the model performance. Regions where models agree with a statistical significance value of > 70 % are marked with sloped black boxes. The CHIRPS datasets have been proven to perform exemplary over the study region following detailed assessment study by various researchers (Kimani et al., 2018, Cattaini et al., 2018; Gebrechorkos et al., 2018; Dinku et al., 2018; Ayugi et al., 2019). To highlight, Dinku et al. (2018) employed > 1200 station datasets to evaluate the CHIRPS and established a higher skill and low or no bias over EA domain.

The results show that MME of CMIP6 can depict the observed spatial distribution of precipitation extremes for both seasons (Figures 2 and 3), albeit some noticeable exceptions in some indices. For instance, the MAM season (Figure 2) underestimates the total precipitation occurrence with ≤ 10% bias while extremely wet days are overestimated in model ensemble. Interestingly, there were also differences in the estimations of consecutive dry days or wet days during the study period. Significant biases are depicted in CWD, with a high magnitude of ≥ 160 % covering the whole region. The observed declining trends in the seasonal precipitation over the region is not well captured by the MME, leading to huge biases noted. In agreement with previous studies (i.e., Osima et al., 2018; Ogega et al., 2020), the GCMs show an underestimation of CDD, and R20mm, especially over eastern Kenya and northeastern Tanzania, where model agree significantly. Remarkably, western Uganda shows a substantial bias of overestimating heavy precipitation days despite underestimating in most regions. This could be due to moist westerlies originating from the Congo basin resulting in enhanced rain during this season in the north and southwest when other parts of the country are cold and dry (Mchugh 2004; Kizza et al. 2009).

 doi:10.20944/preprints202101.0112.v1

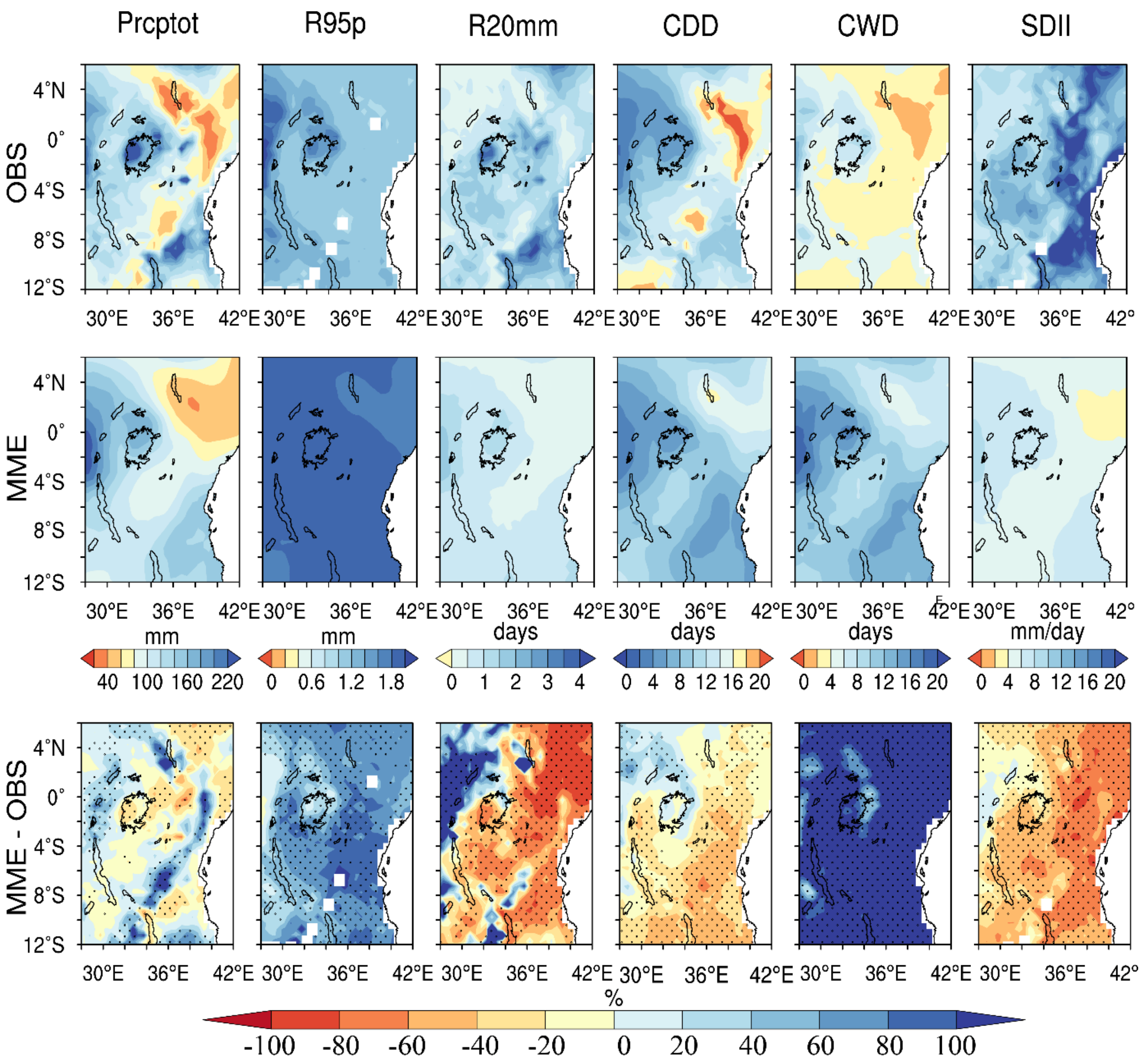

Figure. 2. Spatial distribution of March-April-May (MAM) precipitation extremes, (left)–(right) PRCPTOT, R95p, R20mm, CDD, CWD, and SDII from (top)–(bottom) CHIRPS (OBS), Ensemble Mean (MME), and percentage bias of the MME relative to OBS for the present-day period, 1995–2014. The black dots indicate statistically significant changes at the 95% confidence level while areas, where 70% of models agree on the changes, are marked with sloped black boxes.

On the other hand, the OND season (Figure 3) demonstrates the incidence of underestimations of CDD, SDII, and R20mm in most regions, except for western Uganda, that depicts significant positive bias of the number of very heavy precipitation days. Conversely, the occurrence of CWD, R95p, and PRCPTOT shows significant overestimations over most regions. Interestingly, similar to the MAM season, the consecutive wet days are strongly overestimated with bias > 160 %, which is substantial in most areas. This depicts the inability to models to reflect the recent drying patterns observed over the study region since 1999 (Lyon and DeWitt, 2012, Lyon, 2014). Previous studies have established the causes of observed drying patterns attributed to the western Indian Ocean (William and Funk, 2011).

Overall, the MME of CMIP6 simulates the spatial patterns of daily precipitation extremes reasonably well over the study region. Most models show the higher distribution of precipitation along the western side of the study area and dry bias and the eastern Kenya and parts of Tanzania. Except for CWD, most indices are well represented over the study region, thereby giving the model ensemble confidence to be employed to projection extreme events over the study area.

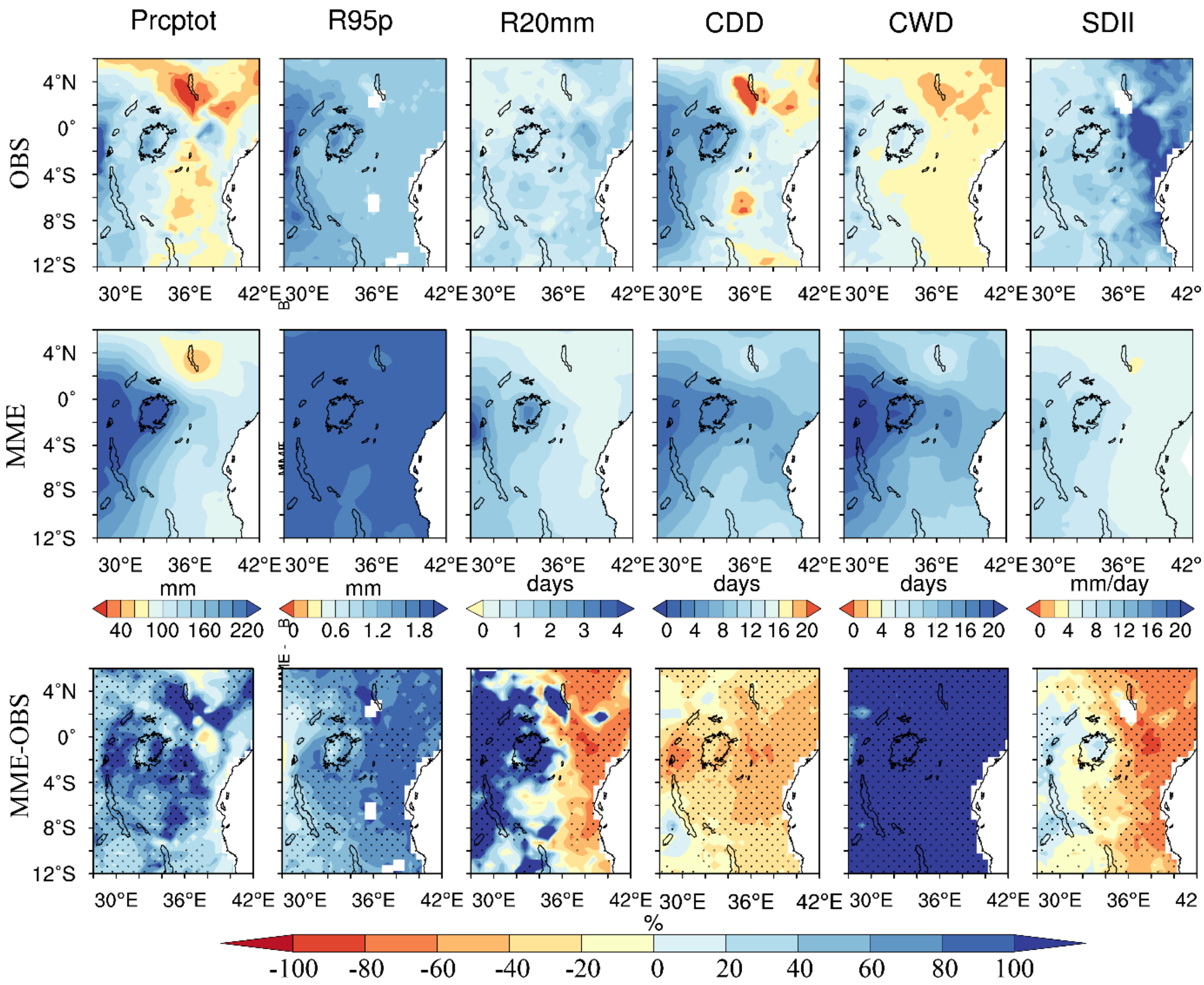

Figure. 3. Spatial distribution of October-November-December (OND precipitation extremes, (left)–(right) PRCPTOT, R95p, R20mm, CDD, CWD, and SDII from (top)–(bottom) CHIRPS (OBS), Ensemble Mean (MME), and percentage bias of the MME relative to OBS for the present-day period, 1995–2014. The black dots indicate statistically significant changes at the 95% confidence level while areas, where 70% of models agree on the changes, are marked with sloped black boxes.

3.1 Seasonal precipitation distributions

3.1.1 MAM precipitation extremes

The overarching objective of climate projection is to equip society and local communities with timely and relevant information about future changes in weather and climate. Consequently, the present study considered relevant extreme indices suitable for examining the societal needs that are "user-relevant" for appraising possible future changes in extreme events. Figures 4 and 5 present spatial distribution of the projected changes in MAM precipitation extremes under the SSP2 – 4.5 (SSP5 – 8.5) scenarios for the near future (2021 - 2040) relative to 1995–2014. The region will experience varying changes over the next few decades. For illustration, the results show that the area will experience a significant occurrence of extreme wet days that is projected to occur over the whole region. The projected upsurge range between 0.2 – 0.6 mm in both scenarios.

Further, analysis shows an increase in total PRCPTOT during the SSP5 – 8.5 scenario compared to the SSP2 – 4.5 scenario. The projection for modest mitigation (Figure 4) demonstrate a declining trend over Kenya and Uganda while significant increase tendency is noted over the Tanzania region. Notably, no significant differences are projected to occur in wet-day intensity index (SDII), both in SSP2 – 4.5 or in worst-case, no policy (i.e., SSP5 – 8.5) scenario. The CWD index, CDD, and R20mm equally show no significant changes in the two scenarios projected (Figures 4 and 5). The occurrence of heavy precipitation days is likely to intensify over the Tanzania region during SSP2 – 4.5 and further strengthen to cover other areas such as western Kenya and northwest Uganda. A recent study (Mafuru and Guirong, 2020) noted an increase of heavy rainfall events (HRE) with a total of 822 cases, which were mostly concentrated over the northern section of Tanzania. The study further attributed the upsurge in HREs to several factors such as low-level westerly convergence, intensified advection of moisture from both the Indian Ocean (IO) and Congo basin, and distinct tropospheric warm temperature anomaly. The results of the present study suggest that the region will continue to experience changes in extreme weather and climate events. Most indices demonstrate the reduction in extreme incidences, except for total precipitation and the variability in very wet days (R95p). Such changes will likely affect most sectors, such as agricultural productivity and societal infrastructure.

 doi:10.20944/preprints202101.0112.v1

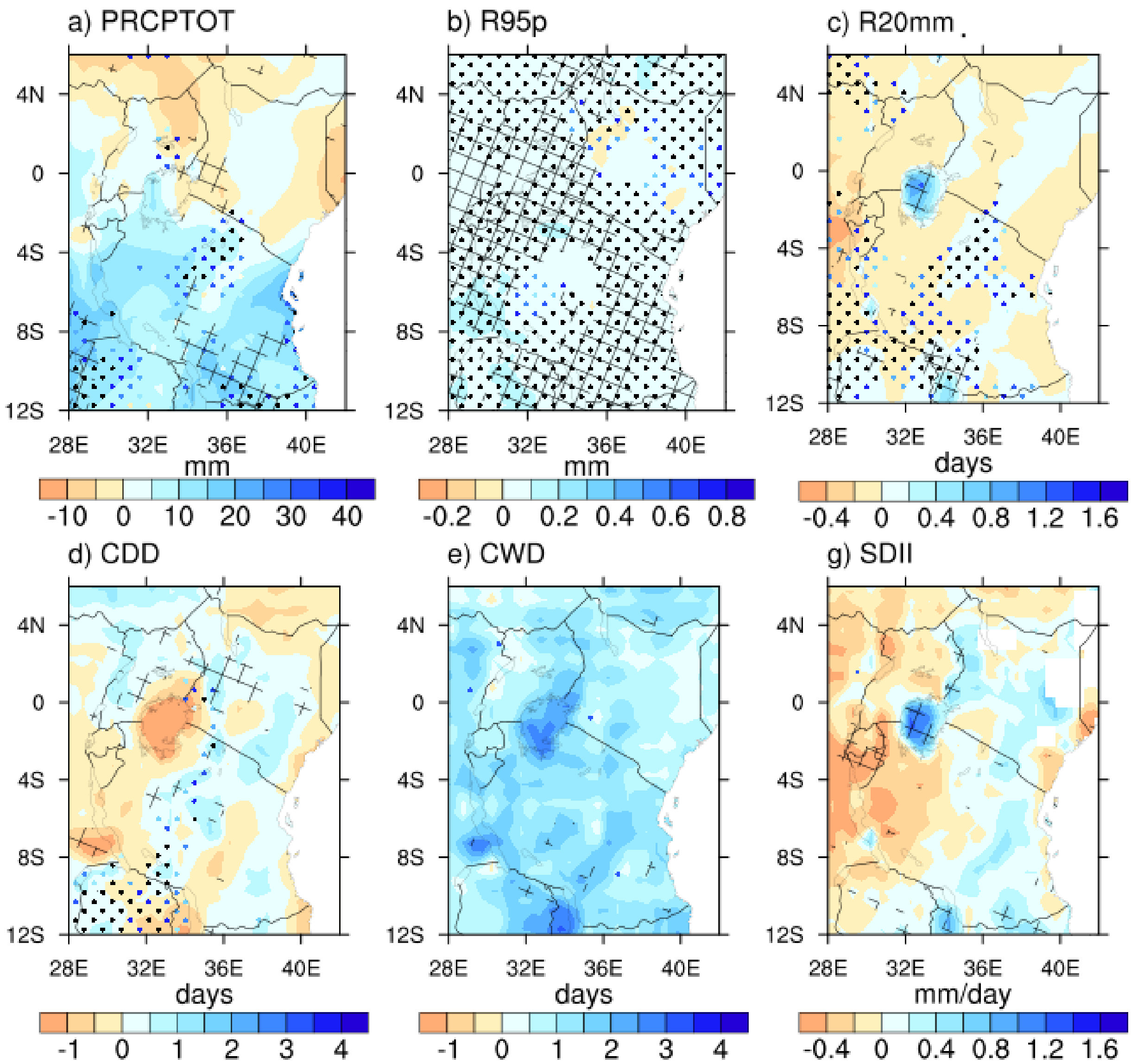

Figure 4. Spatial distribution of the projected changes in March-April-May (MAM) precipitation extremes under the SSP2-4.5 scenario for the near future (2021-2040) relative to 1995–2014. The black dots indicate statistically significant changes at the 95% confidence level while areas, where 70% of models agree on the projected changes, are marked with sloped black boxes.

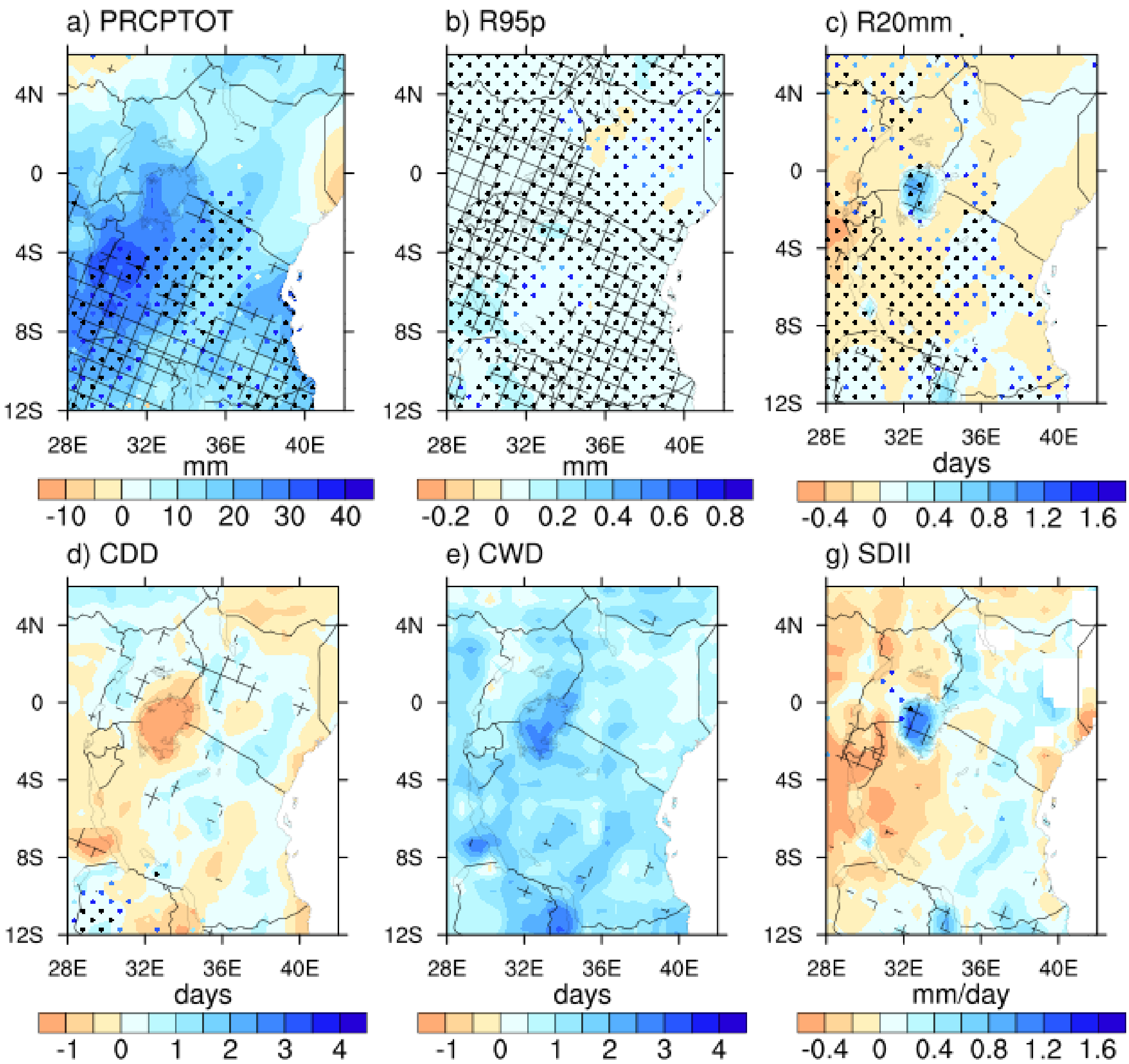

Figure 5. Spatial distribution of the projected changes in March-April-May (MAM) precipitation extremes under the SSP5-8.5 scenario for the near future (2021-2040) relative to 1995–2014. The black dots indicate statistically significant changes at the 95% confidence level while areas, where 70% of models agree on the projected changes, are marked with sloped black boxes.

Projected changes towards the end of the century (i.e., 2081 – 2100) relative to 1995 – 2014 is for the long rainy season is presented in Figure 6 (SSP2 – 4.5) and Figure 7 (SSP5 – 8.5). Because of the adverse impacts of extreme events, it is essential to examine its evolution both in the near future and towards the end of the century for adequate planning purposes. Moreover, the large-scale climate drivers regulating the interannual and decadal variability of precipitation over the region for the MAM season remains complex (Lyon and DeWitt, 2012; Yang et al., 2014). Assessment of the number of wet days and simple precipitation index are represented by PRCPTOT and SDII. The results (Figures 6 and 7) show a significant increase in total precipitation in wet days (RR ≥ 1mm) covering the entire area with a substantial magnitude of > 40 mm impacting the southwestern parts of Tanzania, southern Uganda and along parts of western Kenya. Noticeably, during the SSP2 – 4.5 scenario, the spatial patterns of PRCPTOT depict the considerable impact over southwest and southeast Tanzania while during the SSP5 – 8.5, significant shift is noted towards the southwest section only. Conversely, the intensity index depicts no remarkable change in both scenarios towards the end of the century. The spatial distribution shows comparable patterns with Uganda and along the southeast stretch of Kenya and Tanzania, highlighting significant impact with most models agreeing to the projected changes. The projected SDII change under the SSP5 – 4.5 scenario show 0.4 – 1.6 mm, while SSP5 – 8.5 depicts a 0.8 – 1.6 mm increase towards the end of the century.

Further analyses on the duration indices, which mainly defines periods of excessive wetness/dryness such as CDD and CWD, show continuous drying (wetting) patterns during the two scenarios examined. The CDD depicts significant drying patterns over Kenya and few areas along with southern parts of Tanzania during SSP2 – 4.5 and 5 – 8.5 scenarios. Similar patterns are shown for CWD during the study period but for wetting trends. Besides, the study considered R95p and R20mm to examine the evolution of the number of days with heavy precipitation and projected changes in total rainfall with >95th percentile. The two indices' results depicted noteworthy positive trajectories over the whole region with values of 0.2 – 0.4 mm (R95p) and 0.4 – 1.4 mm (R20mm) during the two scenarios.

Overall, the study area will experience varying extremes, such as a reduction in PRCPTOT under 'business as usual' scenario than a modest mitigation policy scenario. A decrease in MAM precipitation could be due to projected earlier onset/cessation dates relative to the baseline period, possibly impacting the long rain season (Ogega et al., 2020). Likewise, the persistent drying patterns are showed in CDD, which is likely to intensify under the SSP5 – 8.5 scenario. The resultant impact will likely to be reduced agricultural production which mainly relies on rainfall and other climatic variables. Precipitation intensity will likely to increase with cases of R95p, R20mm, and CWD, showing significant positive projections. The incidences of concurrent wetness/dryness projected agree with previous studies (Shongwe et al., 2011; Liebman et al., 2014; Maidment et al., 2015). The region is prone to the occurrence of drought/flood incidences, which are mainly a result of anthropogenic influence and changes associated with internal variability, e.g., by ENSO and in Interdecadal Pacific Oscillation (IPO) (Gu et al., 2013; Lyon, 2014; Hua et al., 2016; Dai, 2016).

 doi:10.20944/preprints202101.0112.v1

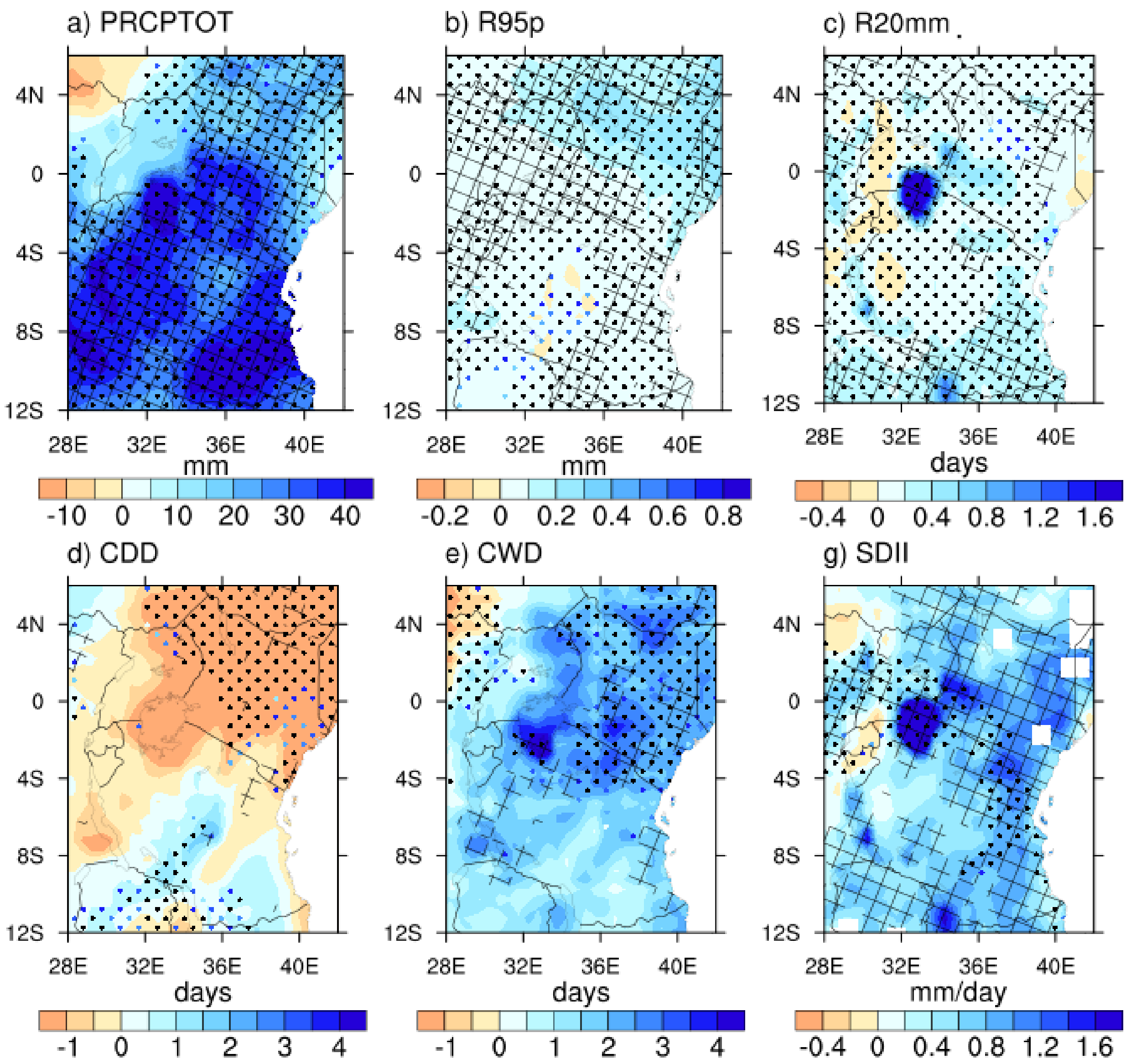

Figure 6. Spatial distribution of the projected changes in March-April-May (MAM) precipitation extremes under the SSP2-4.5 scenario for the Far future (2081-2100) relative to 1995–2014. The black dots indicate statistically significant changes at the 95% confidence level while areas, where 70% of models agree on the projected changes, are marked with sloped black boxes.

 doi:10.20944/preprints202101.0112.v1

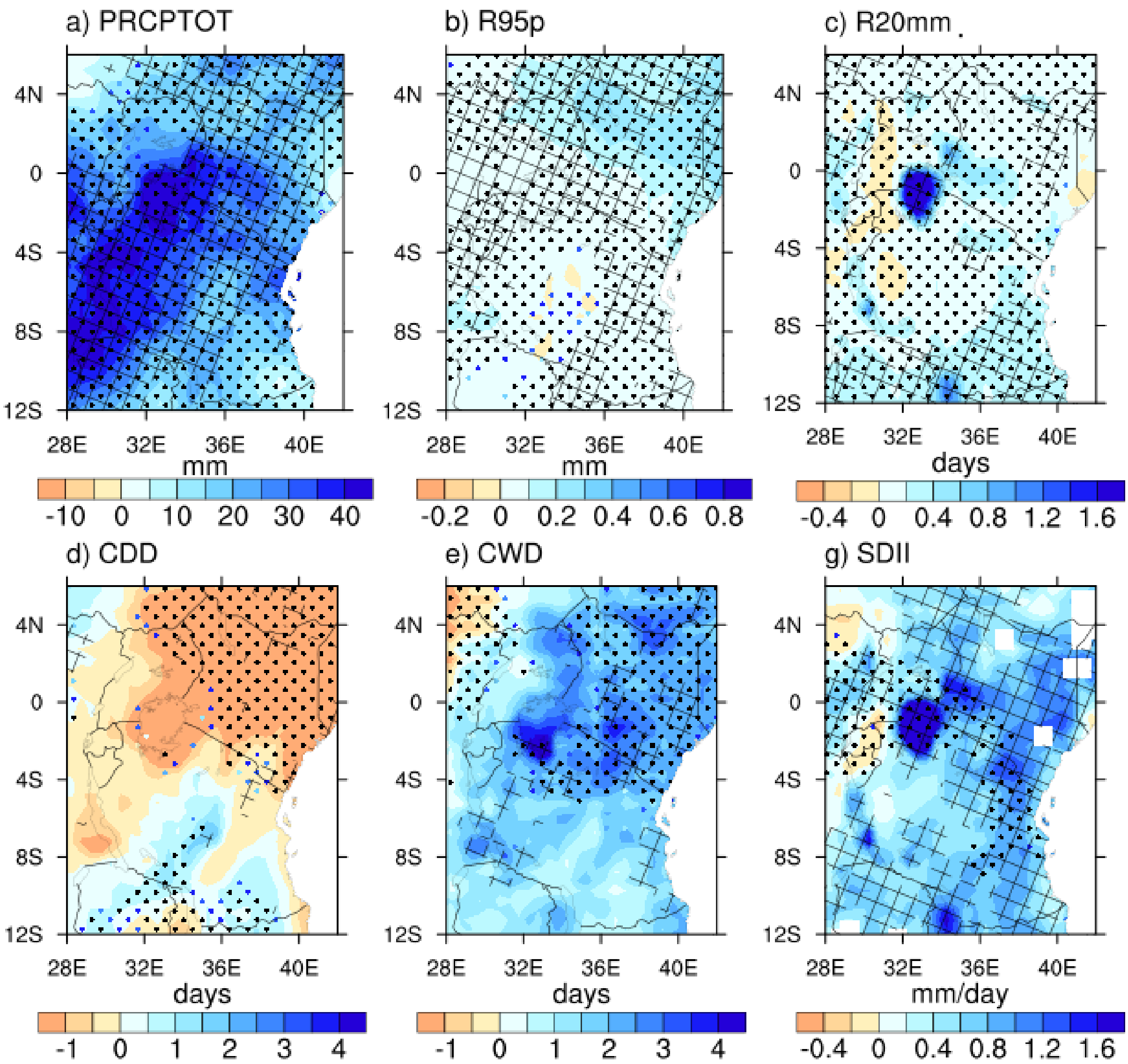

Figure 7. Spatial distribution of the projected changes in March-April-May (MAM) precipitation extremes under the SSP5-8.5 scenario for the Far future (2081-2100) relative to 1995–2014. The black dots indicate statistically significant changes at the 95% confidence level while areas, where 70% of models agree on the projected changes, are marked with sloped black boxes.

3.1.2 OND precipitation extremes

Recent studies have shown that EA region is likely to experience a massive increase in precipitation occurrence during OND season as compared to MAM season (Maidment et al., 2015; Ongoma et al., 2019; Tan et al., 2020). Understanding the evolution of extreme events in the wake of the projected increase in precipitation remains a crucial task. This study assessed the changes in extreme during period 2021 – 2040 and towards the end of century 2081 – 2100 for two scenarios SSP2 – 4.5 and 5 – 8.5. Figures 8 and 9 displays the spatial distribution of the projected changes during OND season under two main scenarios utilized in this study. The results for extreme indices show no significant change in the two scenarios employed. For instance, projections for PRCPTOT (Figure 8) display intensification variations along with western Uganda with > 40 mm while reduction trends (< -10 mm) are observed over Tanzania region. Corresponding patterns are detected during SSP5 – 8.5 scenario (Figure 9). Regarding the projected changes in R95p, the MME demonstrate an agreement of 70 % in likely changes over the entire EA region with reported changes of about 0.2 – 0.4 mm in both figures 8 and 9. Notable increasing trends are recorded in CDD over entire Kenya while southern parts of Tanzania depict likelihood of reduction trends, evidenced by most models agreement. Likewise, the CWD projections exhibit tendencies of intense occurrence around Lake Victoria region whereas no significant changes are observed are over most parts, except for the southern parts of Tanzania where a reduction of up to 4 days in a year is projected. The findings of the present study are in harmony with the recent study that employed large ensemble members from regional climate models (RCMs) models outputs to project changes in extremes precipitation over EA region (Cattaini et al., 2018; Osima et al., 2018; Ogega et al., 2020). Studies above noted an increase(decrease) in CDD (CWD) over the study domain which is mainly associated with the alteration in the Hadley circulations and thermodynamic components such as Indian Ocean Dipole (IOD) (Hastenrath et al., 2011; Endris et al., 2016, 2019).

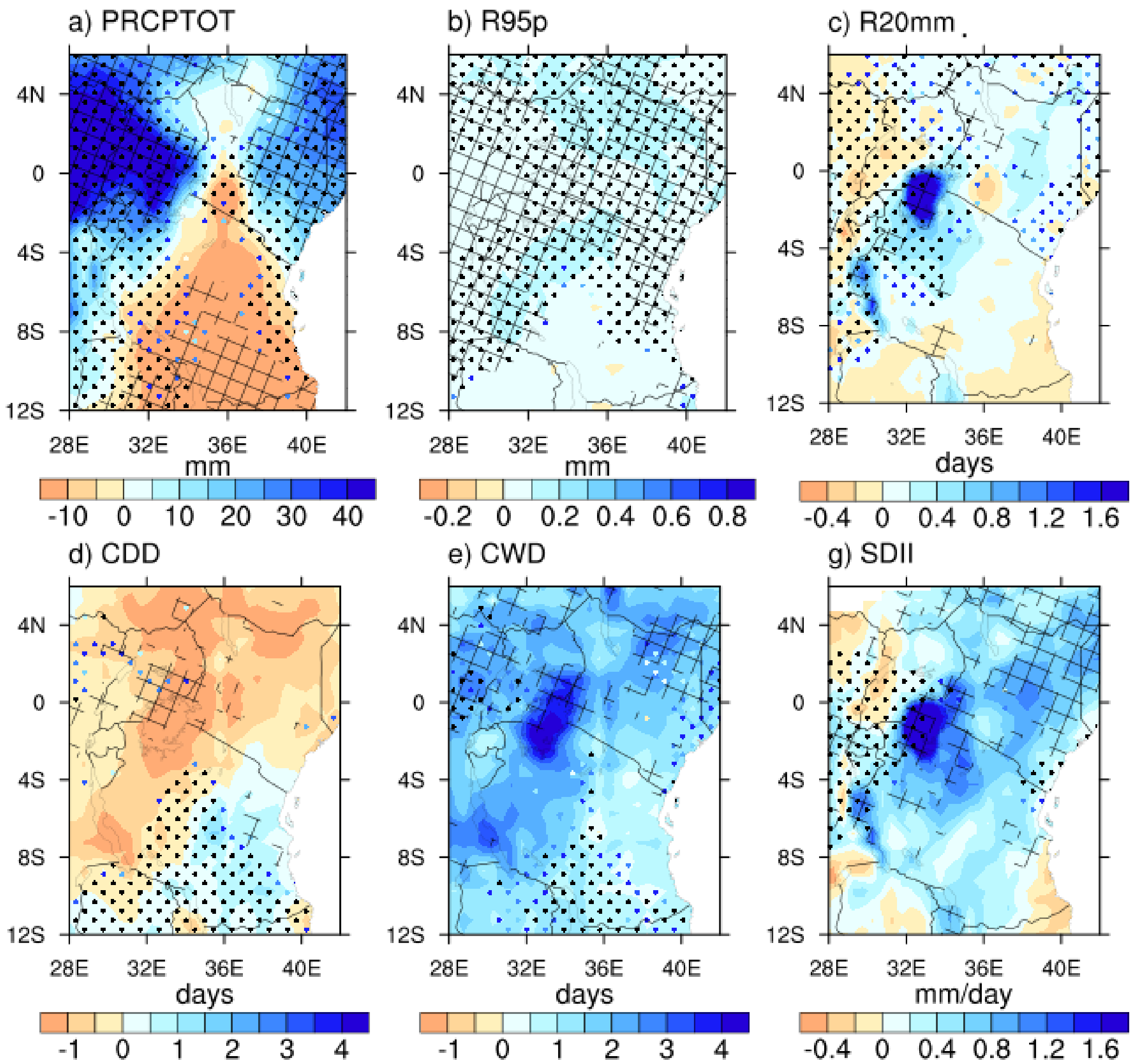

Figure 8. Spatial distribution of the projected changes in October-November-December (OND) precipitation extremes under the SSP2-4.5 scenario for the near future (2021-2040) relative to 1995–2014. The black dots indicate statistically significant changes at the 95% confidence level while areas, where 70% of models agree on the projected changes, are marked with sloped black boxes.

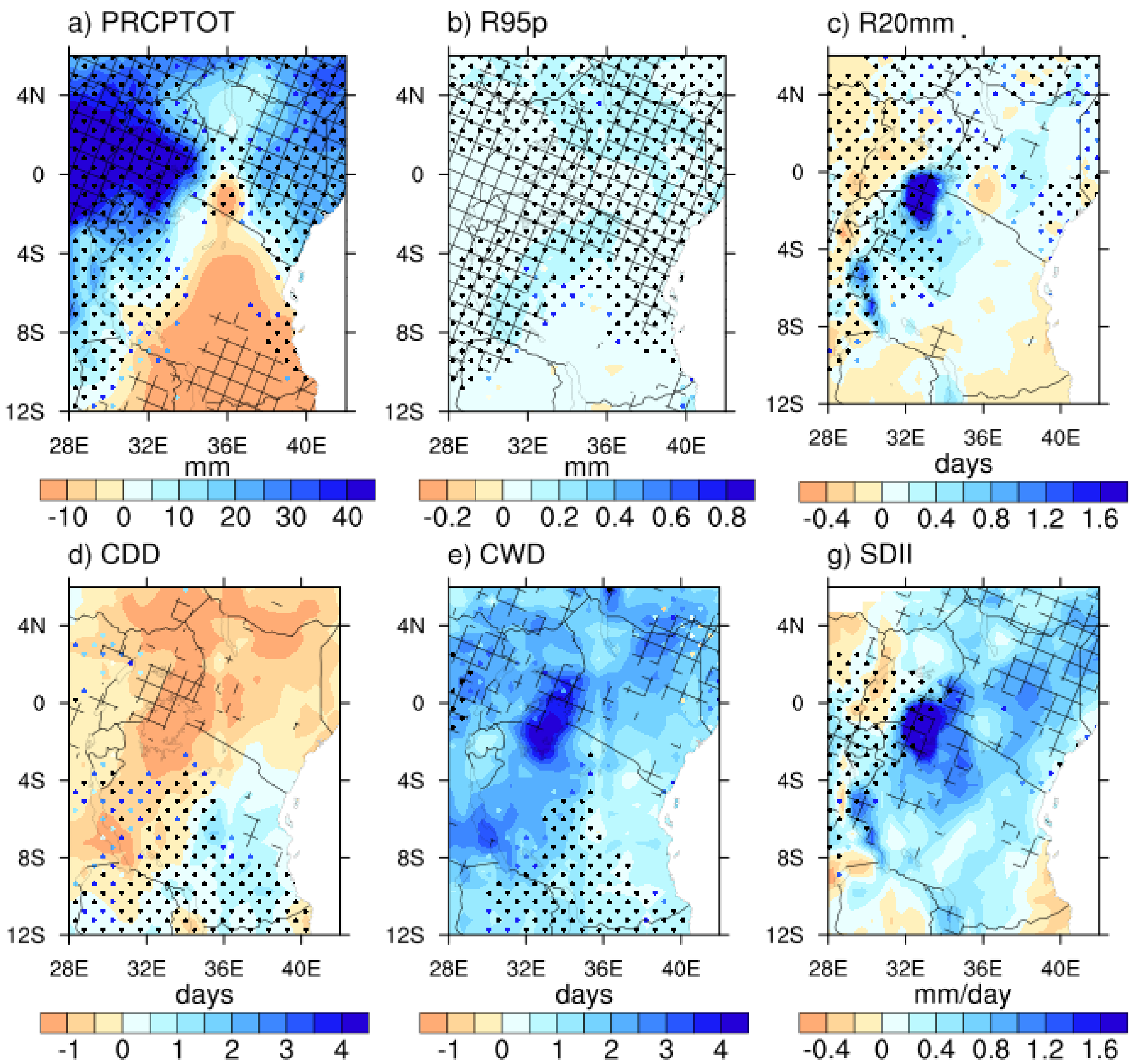

Figure 9. Spatial distribution of the projected changes in October-November-December (OND) precipitation extremes under the SSP5-8.5 scenario for the near future (2021-2040) relative to 1995–2014. The black dots indicate statistically significant changes at the 95% confidence level while areas, where 70% of models agree on the projected changes, are marked with sloped black boxes.

The projections showing probable changes towards the end of the twenty-first century are presented in figures 10 and 11. The figures show likely deviations in OND precipitation extremes under the SSP2 – 4.5 scenario relative to the baseline period. Undoubtedly, the results show an intense incidence of projected SDII, PRCPTOT and CWD over entire Kenya and Uganda. At the same time, the sharp decline is anticipated over southern parts of Tanzania (Figures 10 and 11). Reverse trends are showed CDD which indicate significant drying scenario over Kenya and Uganda while southern Tanzania exhibits fewer incidences of CDD.

The rise in CDD, the decline in CWD and the general increase in SDII may suggest the likelihood of less rainy days with regular precipitation above average. These findings pose a challenge to farming activities and, thus, to the socio-economic well-being of EA societies whose economy is heavily powered by small-scale rain-fed agriculture production (Adhakari et al., 2015; Mumo et al., 2018).

The tendencies of R95p and R20mm signifying percentile-based and threshold indexes show a remarkable increase in the projected precipitation. The observed rise in both parameters (Figures 10 and 11) are mainly centred around inland lake region with values of 0.2 – 0.4 mm (0.4 – 1.6 days) for R95p (R20mm), respectively. Presence of complex physiographical features has considerable influence on the variation of extreme events and impacted regions (Nicholson and Kim, 1997; Camberlin, 2018). For instance, the presence of large inland water bodies, ie. Lake Victoria, which is the largest freshwater lake in Africa and second in the world covering about 68000 km^2 and bordering three countries; Uganda (45 %), Tanzania (49 %) and Kenya (6 %) have a significant influence on the incidences of extreme events (Bowden, 2007). Additionally, high elevation (i.e., Mt. Kenya (5000 m); Mt. Kilimanjaro (5892 m); Mt. Elgon (4321 m) and Mt. Ruwenzori (5109 m)) among others impact hugely on precipitation extreme. Remarkably, the shift in a projected increase in regions of northeastern Kenya, which is predominantly arid and semi-arid (ASAL) presents an excellent opportunity for agricultural activities that have been deprived due to unbearable climatic conditions.

Preprints (www.preprints.org) | NOT PEER-REVIEWED | Posted: 6 January 2021 doi:10.20944/preprints202101.0112.v1

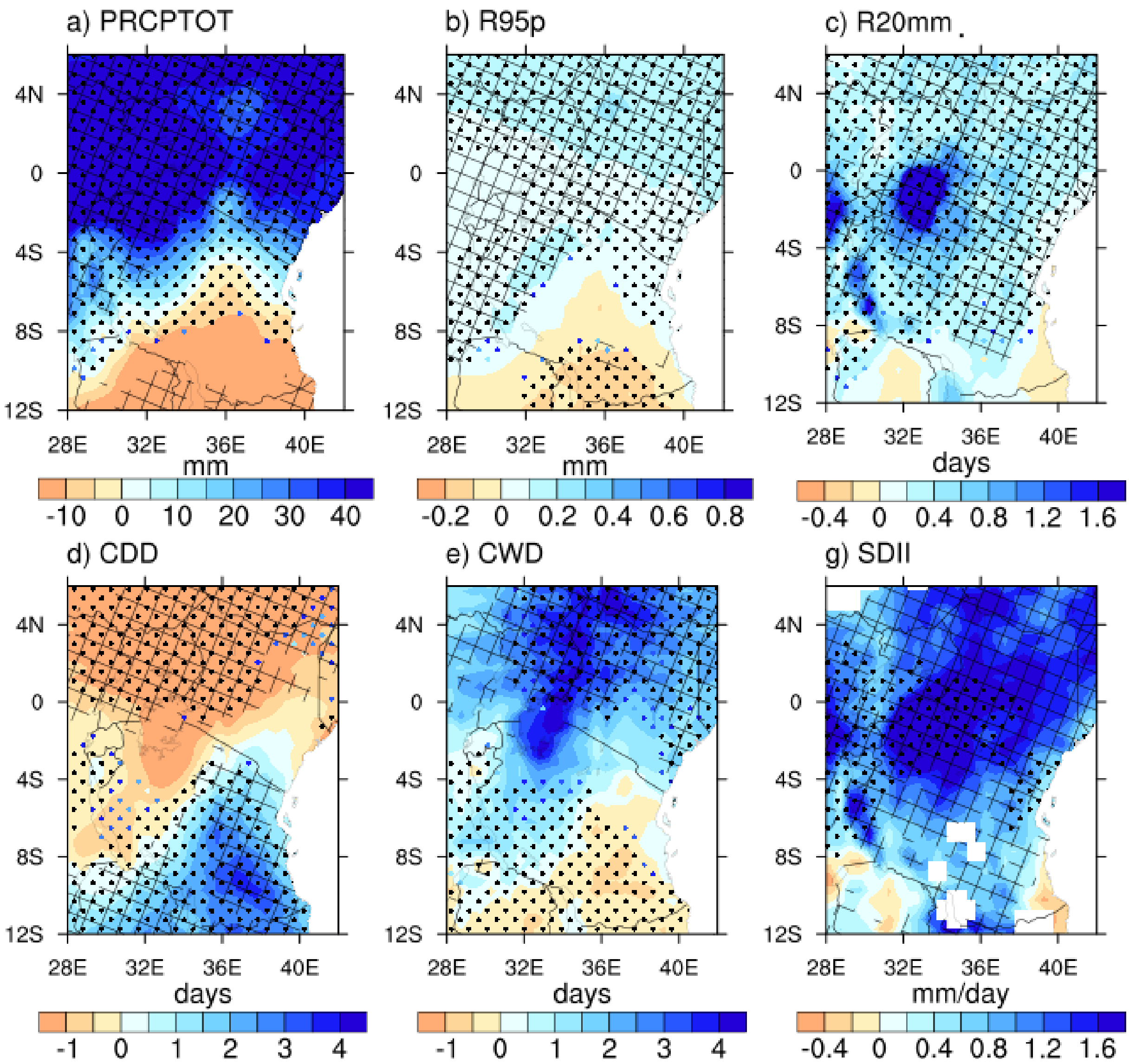

Figure 10. Spatial distribution of the projected changes in October-November-December (OND) precipitation extremes under the SSP2-4.5 scenario for the far future (2081-2100) relative to 1995–2014. The black dots indicate statistically significant changes at the 95% confidence level while areas, where 70% of models agree on the projected changes, are marked with sloped black boxes.

 doi:10.20944/preprints202101.0112.v1

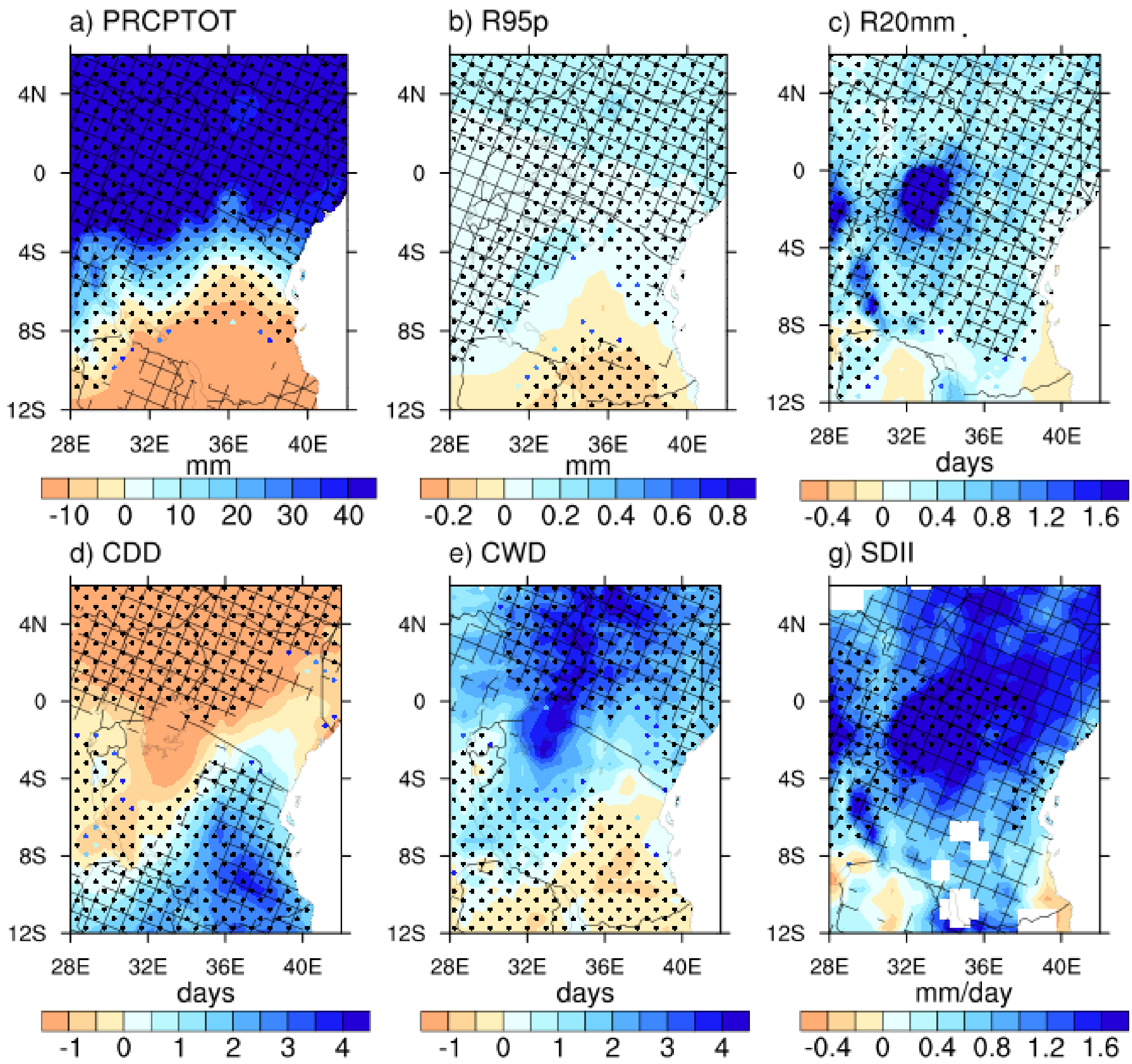

Figure 11. Spatial distribution of the projected changes in October-November-December (OND) precipitation extremes under the SSP5-8.5 scenario for the far future (2081-2100) relative to 1995–2014. The black dots indicate statistically significant changes at the 95% confidence level while areas, where 70% of models agree on the projected changes, are marked with sloped black boxes.

4. Summary and Conclusion

This study sort to examine the future changes of seasonal precipitation extremes over EA region using MME derived from fifteen models' outputs of CMIP6. The research employed subset of precipitation indices provided by ETCCDMI to assess extreme incidences during two time slices defined as near future (2021 – 2040) and far future (2081 – 2100). The two main projection utilized is drawn from Tier 1 ScenarioMIP: SSP2 – 4.5 and SSP5 – 8.5. Firstly, the study examined MME's capability to simulate the observed extreme events over the study area for the period 1995 – 2014 using CHIRPS as the observed datasets. Our results show that MME of CMIP6 models can depict the observed spatial distribution of precipitation extremes for both seasons, albeit some noticeable exceptions in some indices. For instance, the CMIP6 ensemble generally depicted large biases of CWD overestimation during the MAM and OND season, respectively.

In agreement with previous studies (e.g., Ongoma et al., 2018c; Osima et al., 2018; Ayugi et al., 2019), this study's findings yield considerable confidence in CMIP6 to be employed for projection of extreme events over the study area. Analysis of extreme estimations shows an increase (decrease) in CDD(CWD) during 2081 – 2100 relative to the baseline period in both seasons. Moreover, SDII, R95p, R20mm, and PRCPTOT demonstrate significant OND estimates compared to the MAM season. The spatial variation for extreme incidences shows likely intensification over Uganda and most parts of Kenya, while reduction is observed over the Tanzania region. The increase in projected extremes during two main rainfall seasons poses a significant threat to the sustainability of societal infrastructure and ecosystem wellbeing. On the other hand, it is imperative to note that the predominantly ASALs and are estimated to experience wet conditions. This will provide the new opportunity for agricultural and other economic activities. The projected drying patterns over the Tanzanian belt call for a new policy formulation and possible mitigation measures to cushion the community from possible impacts of drought events that are likely to ravage the region. The results from these analyses present an opportunity to understand the emergence of extreme events and the capability of model outputs from CMIP6 in estimating the projected changes. More studies are encouraged to examine the underlying physical features modulating the occurrence of extremes incidences projected for relevant policies.

Competing interests: No competing interest in the present study among the authors or any other body.

Authors contributions: All authors made an equal contribution to the manuscript's development and consented to the submission for publication in the esteemed journal of theoretical and applied climatology. The following are individual contributions: Brian Ayugi: conceptualization, formal writing, funding, original draft preparation. Victor Dike: Data curation, methodology, visualization. Hamida Ngoma: writing-review and editing, investigation. Hassen Babaousmail: methodology, investigation, data curation. Victor Ongoma: Validation, writing-review, and editing.

Funding

Financial and material support received from National Key Research and Development Program of China (Grant No. 2017YFA0603804 and 2018YFC1507704), National Science Foundation of China (No. 41805048) is vastly appreciated.

Compliance with ethical standards

Authors agreed to a unanimous correspondence for the publication of the manuscript.

Availability of data and materials: Data and materials will be made available upon request. Authors agreed to a unanimous correspondence for the publication of the manuscript.

References

Adhikari, U., Nejadhashemi, A.P., Woznicki, S.A., 2015. Climate change and Eastern Africa: a review of impact on major crops. Food Energ. Secur., 4: 110–132. doi:10.1002/fes3.61

Akinsanola, A.A., Zhou, W., 2019. Projections of West African summer monsoon rainfall extremes from two CORDEX models *Clim. Dyn.* 52 2017.dio. 10.1088/1748/1748-9326/ab92cl

AghaKouchak, A., Chiang, F., Huning, L.S., Love, C.A., Mallakpour, I., Mazdiyasni, O., Moftakhari, H., Papalexiou, S.M., Ragno, E., Sadegh, M., 2020. Climate Extremes and Compound Hazards in a Warming World. Annu. Rev. Earth Planet. Sci. 48.20.1-20.30

Aguilar, E., Barry, A.A., Brunet, M., Ekang, A., Fernandes, A., Massoukina, M., Mbah, J., Mhanda, D., Nascimento, J., Peterson, T.C., Umba, T., Tomou, M., Zhang, X., 2009 Changes in temperature and precipitation extremes in western central Africa, Guinea Conakry, and Zimbabwe, 1955–2006 J. Geophys. Res. Atmos. 114 D02115.dio. 10.1029/2008JDO11010

Alexander, L.V,, Zhang, X., Peterson, T.C., Caesar, J., Gleason, B., Klein Tank, A.M.G, Haylock, M., Collins, D., Trewin, B., Rahimzadeh, F., Tagipour, A., Kumar, K.R., Revadekar, J., Griffiths, G., Vincent, L., Stephenson, D.B., Burn, J., Aguilar, E., Brunet, M., Taylor, M., New, M., Zhai, P., Rusticucci, M., Vazquez-Aguirre, J.L., 2006. Global observed changes in daily climate extremes of temperature and precipitation. J. Geophys. Res. Atmos.,111, D05109. doi:10.1029/2005JD006290

Alexander, L.V., 2016. Global observed long-term changes in temperature and precipitation extremes: A review of progress and limitations in IPCC assessments and beyond. Weather Clim. Extrem.11, 4-16. https://doi.org/10.1016/j.wace.2015.10.007

Ayugi, B.O., Tan, G., 2019. Recent trends of surface air temperatures over Kenya from 1971 to 2010. Meteorol. Atmos. Phys.,131, 1401-1413 https://doi.org/10.1007/s00703-018-0644-z

Ayugi, B., Tan, G., Ullah, W., Boiyo, R., Ongoma, V., 2019. Inter-comparison of remotely sensed precipitation datasets over Kenya during 1998–2016. Atmos. Res. 225 (1), 96–109.https://doi.org/10.1016/j.atmosres.2019.03.032

Ayugi, B., Tan, G., Gnitou, G.T., Ojara, M., Ongoma, V., 2020a. Historical evaluations and simulations of precipitation over Eastern Africa from Rossby Centre Regional Climate Model. Atmos. Res. 232. https://dio.org/10.1016.jatmosres.2019.104705

Ayugi, B., Tan, G., Niu, R., Babaousmail, H., Ojara, M., Wido, H., Mumo, L., Nooni, I., Ongoma, V., 2020b. Quantile Mapping Bias Correction on Rossby Centre Regional Models Climate Models for Precipitation Analysis over Kenya, East Africa. *Water*. 2020b,*12*,801; https://dio.org/10.3390/w120801

Bowden, R., 2007. Kenya, 2nd edition. Evan Brothers, London, UK.

Camberlin, P., 2018. Climate of Eastern Africa (Vol. 1). Oxford Research Encyclopedia of Climate Science. https://doi.org/10.1093/acrefore/9780190228620.013.512

Cattani, E., Merino, A., Guijarro, J. A., Levizzani, V., 2018. East Africa Rainfall trends and variability 1983-2015 using three long-term satellite products. Remote Sens, 10, 1–26. https://doi.org/10.3390/rs10060931

Chai, T., Draxler, R. R., 2014. Root mean square error (RMSE) or mean absolute error (MAE)? -Arguments against avoiding RMSE in the literature. Geosci. Model Dev., 7, 1247–1250. doi.org/10.5194/gmd-7-1247-2014

Chen, H., Sun, J., 2018. Projected changes in climate extremes in China in a 1. 5ºC warmer worlds. China. Int. J Climatol., 127, 393-407. Dio 10.1002/joc.5521

Collins, M., Knutti, R., Arblaster, J., Dufresne, J.-L., Fichefet, T., Friedlingstein, P., Gao, X., Gutowski, W.J., Johns, T., Krinner, G., Shongwe, M., Tebaldi, C., Weaver, A. J., Wehner, M., 2013. Long-term climate change: projections, commitments and irreversibility. In: Stocker, T.F., Qin, D., Plattner, G.-K., Tignor, M., Allen, S.K., Boschung, J., Nauels, A., Xia, Y., Bex, V., Midgley, P.M. (Eds.), Climate Change 2013: The Physical Science Basis. Contribution of Working Group I to the Fifth Assessment Report of the Intergovernmental Panel on Climate Change. Cambridge University Press, Cambridge, United Kingdom and

New York, NY, USA

Dai, A., 2016. Future Warming Patterns Linked to Today's Climate Variability. Sci Rep,*6*, 6–11. https://doi.org/10.1038/srep19110

Dinku, T., Funk, C., Peterson, P., Maidment, R., Tadesse, T., Gadain, H. and Ceccato, P., 2018. Validation of the CHIRPS satellite rainfall estimates over eastern Africa. Q J R Meteorol Soc, 144, 292–312. https://doi.org/10.1002/qj.3244

Donat, M., Alexander, L.V., Yang, H., Durre, I., Vose, R., Dunn, R.J.H., Willett, K.M., Aguilar, E., Brunet, M., Caesar, J., Hewitson, B., Jack, C., Klein Tank, A.M.G., Kruger, A.C, Marengo, J., Peterson, T.C., Renom, M., Oria Rojas, C., Rusticucci, M., Salinger, J., Elrayah, A.S., Sekele, S.S., Srivastava, A.K., Trewin, B., Villarroel, C., Vincent, L.A., Zhai, P., Zhang, X., Kitching, S., 2013. Updated analyses of temperature and precipitation extreme indices since the beginning of the twentieth century: the HadEX2 dataset. J. Geophys. Res., 118: 2098–2118. doi:10.1002/jgrd.50150

Eckstein, D., Künzel, V., Schäfer, L., Winges, M., 2020. Global Climate Risk Index 2020. Bonn: Germanwatch.

Endris, H.S., Lennard, C., Hewitson, B., Dosio, A., Nikulin, G., Panitz, H.J., 2016. Teleconnection responses in multi-GCM driven CORDEX RCMs over Eastern Africa. Clim dyn, 46, 2821-2846. DOI 10.1007/s00382-015-2734-7

Endris, H.S., Lennard, C., Hewitson, B., Dosio, A., Nikulin, G., Artan, G.A., 2019. Future changes in rainfall associated with ENSO, IOD and changes in the mean state over Eastern Africa. Clim dyn, 52, 2029-2053. https://doi.org/10.1007/s00382-018-4239-7

Eyring, V., Bony, S., Meehl, G.A., Senior, C.A., Stevens, B., Stouffer, R.J., Taylor, K.E., 2016. Overview of the coupled model Intercomparison project phase 6 (CMIP6) experimental design and organization. Geosci. Model Dev. (GMD) 9, 1937–1958. https://doi.org/10.5194/gmd-9-1937-2016.

FAO., 2019. The state of Food Security and Nutrition in the World 2019. Safeguarding against economic slowdowns and downturns. Rome, FAO. Licence: CC BY-NC-SA. 3.0 IGO

Fischer, E.M. and R. Knutti, 2016: Anthropogenic contribution to global occurrence of heavy-precipitation and high-temperature extremes. Nat. Clim. Chang, **5(6)**, 560–564, doi:10.1038/nclimate2617.

Funk, C., Shukla, S., Thiaw, W. M., Rowland, J., Hoell, A., McNally, A., Husak, G., Novella, N., Budde, M., Ligard, C.P., Adoum, A., Galu, G., Korecha, D., magadzire, T., Rodriguez, M., Robjhon, M., Bekele, E., Arsenault, K., Peterson, P., Harrison, L., Fuhrman, S., Devenport, F., Landsfield, M., Pedros, D., Jacob, J., Raynolds, C., Reshef, B., Verdin, J.,

2019. Recognizing the Famine Early Warning Systems Network: Over 30 Years of Drought Early Warning Science Advances and Partnerships Promoting Global Food Security. Bulletin of the Bull. Amer. Meteor. Soc, 100(6), 1011-1027. Dio. 10.1175/BAMS0-D-17-0233.1

Funk, C.C., 2012. Exceptional warming in the western Pacific-Indian Ocean warm pool has contributed to more frequent droughts in eastern Africa. Bull. Amer. Meteor. Soc.,93: 1041–1067. doi:10.1175/BAMS-D-12-00021.1

Funk, C., Peterson, P., Landsfeld, M., Pedreros, D., Verdin, J., Shukla, S., Michaelsen, J., 2015. The climate hazards infrared precipitation with stations - A new environmental record for monitoring extremes. Sci. Data, 2, 1–21. doi.org/10.1038/sdata.2015.66.

Gebrechorkos, S. H., Hülsmann, S., Bernhofer, C., 2017. Evaluation of Multiple Climate Data Sources for Managing Environmental Resources in East Africa. Hydro. Earth Syst. Sci., 22, 4547–4564. https://doi.org/10.5194/hess-2017-558

Gebrechorkos, S.H., Hülsmann, S., Bernhofer, C., 2019. Changes in temperature and precipitation extremes in Ethiopia, Kenya, and Tanzania. Int J Climatol 39:18–30. Dio: 10.1002/joc.5777

Giorgi, F., Raffaele, F., Coppola, E., 2019. The response of precipitation characteristics to global warming from climate projections. Earth Syst. Dynam. 10, 73-89. Dio:10.5194/esd-10-73-2019

Gu, G., Adler, R.F., 2013. Interdecadal variability/long-term changes in global precipitation patterns during the past three decades: Global warming and/or pacific decadal variability? Clim Dyn, 40, 3009–3022. https://doi.org/10.1007/s00382-012-1443-8

Hastenrath, S., Polzin, D., Mutai, C., 2011. Circulation mechanisms of Kenya rainfall anomalies. J Climate 24: 404–412. dio:10.1175/2010JCLI3599.1

Hua, W., Zhou, L., Chen, H., Nicholson, S.E., Raghavendra, A., Jiang, Y., 2016. Possible causes of the Central Equatorial African long-term drought. Environ. Res. Lett. 11 (12), 124002.

IPCC., 2013. Climate change 2013: The Physical Science Basis. Contribution of working group I to the fifth Assessment Report of the Intergovernmental Panel on Climate Change. [Stocker TF, Qin D, Plattner G-K, Tignor M, Allen SK, Boschung J, Nauels A, Xia Y, Bex V, Midgley PM (eds)]. Cambridge University Press, Cambridge, United Kingdom and New York, NY, USA, 1535 pp

IPCC, 2014. Climate Change 2014: Synthesis Report. Contribution of Working Groups I, II and III to the Fifth Assessment Report of the Intergovernmental Panel on Climate Change

[Pachauri RK, Meyer LA (eds.)]. IPCC, Geneva, Switzerland, 151 pp.

IPCC., 2018. Global Warming of 1.5° C: An IPCC Special Report on the Impacts of Global Warming of 1.5° C Above Pre-Industrial Levels and Related Global Greenhouse Gas Emission Pathways, in the Context of Strengthening the Global Response to the Threat of Climate Change, Sustainable Development, and Efforts to Eradicate Poverty. Intergovernmental Panel on Climate Change.

Janssen, E., Wuebbles, D. J., Kunkel, K. E., Olsen, S. C., Goodman, A., 2014. Observational-and model-based trends and projections of extreme precipitation over the contiguous United States. Earth's Future, 2, 99-113. Dio. 10.1002/2013ef000185

Jiang, Z.H., Song, J., Li, L.W.L. Chen, Z.F., Wang, J., Wang., 2012. Extreme climate events in China: IPCC-AR4 model evaluation and projection. Climatic Chang, 110, 385–401.

Jiang, Z. H., W. Li, J. J. Xu, et al., 2015: Extreme precipitation indices over China in CMIP5 models. Part I: Model evaluation. J. Climate, 28, 8603-8619, doi: 10.1175/jcli-d-15-0099.1.

Kimani, M.W., Hoedjes, J.C. B., Su, Z., 2017. An assessment of satellite-derived rainfall products relative to ground observations over East Africa. Remote Sens, 9. 430. https://doi.org/10.3390/rs9050430

Kilavi, M., MacLeod, D., Ambani, M., Robbins, J., Dankers, R., Graham, R., Helen, T., Salih, A. A. M., Todd, M.C., 2018. Extreme rainfall and flooding over Central Kenya Including Nairobi City during the long-rains season 2018: causes, predictability, and potential for early warning and actions Atmosphere 9, 472. Dio. 10.3390/atmos9120472

Kizza, M., Rodhe, A., Xu, C.Y., Ntale, HK., Halldin, S., 2009. Temporal rainfall variability in the Lake Victoria Basin in East Africa during the twentieth century. Theor appl climatol 98: 119–135. https://doi.org/10.1007/s00704-008-0093-6

Klein Tank, A.M.G., Zwiers, F.W., Zhang, X., 2009. Guidelines on analysis of extremes in a changing climate in support of informed decisions for adaptation. In: Climate Data and Monitoring WCDMP-No. 72, vol. 1500. WMO-TD No., p. 56

Kharin, V., Flato, G.M., Gillett, N.P., Zwiers, F., Anderson, K.J., 2018: Risks from Climate Extremes Change Differently from 1.5°C to 2.0°C Depending on Rarity. Earth's Future, 6, 704–715, doi:10.1002/2018ef000813

Kunkel, K.E., P.D. Bromirski, H.E. Brooks, T. Cavazos, A.V. Douglas, D.R. Easterling, K.A. Emanuel, P.Ya. Groisman, G.J. Holland, T.R. Knutson, J.P. Kossin, P.D. Komar, D.H. Levinson, and R.L. Smith, 2008: Observed changes in weather and climate extremes. In: *Weather and Climate Extremes in a Changing Climate: Regions of Focus: North America,* *Hawaii, Caribbean, and U.S. Pacific Islands* [Karl, T.R., G.A. Meehl, C.D. Miller, S.J. Hassol, A.M. Waple, and W.L. Murray (eds.)]. Synthesis and Assessment Product 3.3. U.S. Climate Change Science Program,Washington, DC, pp. 35-80

Liebmann, B, Hoerling M.P., Funk, C., Bladé, I., Dole, R.M., Allured, D., Quan, X., Pegion P., Eischeid, J.K., 2014. Understanding Recent Eastern Horn of Africa Rainfall Variability and Change. J. Climate, 27: 8630–8645. doi:10.1175/JCLI-D-13-00714.1

Lyon, B., Dewitt, D.G., 2012. A recent and abrupt decline in the East African long rains. Geophys. Res. Lett.,39, L02702. https://doi:10.1029/2011GL050337

Lyon, B., 2014. Seasonal drought in the Greater Horn of Africa and its recent increase during the March–May long rains. J. Clim. 27, 7953–7975.

Mafuru B.K., and Tan, G., 2019. The Influence of ENSO on the Upper Warm Temperature Anomaly Formation Associated with the March-May Heavy Rainfall Events in Tanzania. Int. J Climatol., 40, 2745-2763. Dio.ord/10.1002/joc.6364

Maidment, R.I., Allan, R.P., Black, E., 2015. Recent observed and simulated changes in precipitation over Africa. Geophys. Res. Lett., 42: 8155–8164. doi:10.1002/2015GL065765.

Min, S.K., Zhang, X., Zwiers, F.W., Hegerl, G.C., 2011. Human contribution to more intense precipitation extremes. Nature 470, 378–381. https://doi.org/10.1038/nature09763.

Mchugh, M.J., 2004. Near-Surface Zonal Flow and East African Precipitation Receipt during Austral Summer. J. Clim 17 4070–4079. https://doi.org/10.1175/1520-0442(2004)017<4070: NZFAEA>2.0.CO;2

Mumo, L., Yu, J., Fang, K., 2018. Assessing Impacts of Seasonal Climate Variability on Maize Yield in Kenya. Int. J. Plant Prod. 12, 1-11. doi:10.1007/s42106-018-0027-x.

Myhre, G., Alterskjær, K., Stjern, C. W., Hodnebrog, Ø., Marelle, L., Samset, B. H., Sillman, J., Schaller, N., Fischer, E., Schulz, M., Stohl, A., 2019. Frequency of extreme precipitation increases extensively with event rareness under global warming. Sci. Rep. *9*, 1-10. Dio. 10.1038/s41498-019-52277-4

Niang, I., Ruppel, O.C., Abdrabo, M.A., Essel, A., Lennard, C., Padgham, J., Urquhart, P., 2014. Africa. In: Climate Change 2014: Impacts, Adaptation, and Vulnerability. Part B: Regional Aspects. Contribution of Working Group II to the Fifth Assessment Report of the Intergovernmental Panel on Climate Change [Barros VR, Field CB, Dokken DJ, Mastrandrea MD, Mach KJ, Bilir TE, Chatterjee M, Ebi KL, Estrada YO, Genova RC, Girma B, Kissel ES, Levy AN, MacCracken S, Mastrandrea PR, White LL (eds.)]. Cambridge University Press, Cambridge, United Kingdom and New York, NY, USA, 1199–1265 pp.

Nicholson, S.E., Kim. J., 1997. The relationship of the El Niño–Southern Oscillation to African rainfall. Int. J. Climatol. 17, 117–135, doi:10.1002/(SICI)10970088(199702)17:2<117::AID-JOC84>3.0.CO;2-O.

Nicholson, S.E., 2017. Climate and climatic variability of rainfall over eastern Africa. Rev. Geophys. 55, 590–635. https://doi.org/10.1002/2016RG000544

Ogega, O.M., Koske, J., Kung'u, J.B., Scoccimarro, E., Endris, H.S., Mistry, M., 2020. Heavy precipitation events over East Africa in a changing climate: results from CORDEX RCMs. Clim. Dyn. 2020. doi.org/10.1007/s00382-020-05309-z.

Omondi, P.A., Awange, J.L., Forootan, E., Ogallo, L.A., Barakiza, R., Girmaw, G.B., Fesseha, I., Kululetera, V., Kilembe, C., Mbati, M.M., Kilavi, M., King'uyu, S.M., Omeny, P.A, Njogu, A., Badr, E.M., Musa, T.A., Muchiri, P., Bamanya, D., Komutunga, E., 2014. Changes in temperature and precipitation extremes over the Greater Horn of Africa region from 1961 to 2010. Int. J. Climatol., 34: 1262–1277. doi:10.1002/joc.3763

Ongoma, V., Chen, H., 2017. Temporal and spatial variability of temperature and precipitation over East Africa from 1951 to 2010. Meteorol. Atmos. Phys. 129, 131–144.https://doi.org/10.1007/s00703-016-0462-0

Ongoma, Victor, Haishan Chen, and George William Omony. 2018a. "Variability of Extreme Weather Events over the Equatorial East Africa, a Case Study of Rainfall in Kenya and Uganda." Theor. Appl. Climatol. 131: 295–308. http://dx.doi.org/10.1007/s00704-016-1973-9.

Ongoma, V., Chen, H., Gao, C., 2018b. Projected Change in Mean Rainfall and Temperature over East Africa based on CMIP5 Models. Int. J. Climatol. 38: 1375–1392 https://doi.org/10.1002/joc.5252

Ongoma ,V., Chen, H., Gao, C., Nyongesa, A.M., Polong, F., 2018c. Future changes in Climate Extreme over Equatorial East Africa based on CMIP5 multimodel ensemble. Nat Hazards 90: 901–920. https://doi.org/10.1007/s11069-017-3079-9.

Ongoma, V., Chen, H., Gao, C., 2019. Evaluation of CMIP5 twentieth century rainfall simulation over the equatorial East Africa. Theor. Appl. Climatol. 135, 893–910.http://doi.org/10.1007/s00704-018-2392-x

Onyutha, C., 2020. Analyses of rainfall extremes in East Africa based on observations from rain gauges and climate change simulations by CORDEX RCMs. Clim Dyn (2020). https://doi.org/10.1007/s00382-020-05264-9

Osima, S., Indasi, V.S., Zaroug, M., Endris, H.S., Gudoshava, M., Misiani, H.O., Dosio, A.,

2018. Projected Climate over Greater Horn of Africa under 1.5°C and 2°C global warming. Environ. Res. Lett.13, 6. https://doi.org/10.1128/JVI.74.13.6223-6226.2000

O'Neill, B.C., Tebaldi, C., Vuuren, D.V., Erying, V., Fridelingstein, Hurtt, G., Knutti, R., Kriegler, E., Lamarque, J.F., Lowe, J., Meehl, J., Moss, R., Riahi, K., Sanderson, B.M., 2017. The roads ahead: Narratives for shared socioeconomic pathways describing world futures in the 21st century. Global Environ. Chang., 42, 169–180. https://doi.org/10.1016/j.gloenvcha.2015.01.004.

Papalexiou, S.M., Montanari, A., 2019. Global and regional increase of precipitation extremes under global warming. Water Resour Res, *55*, 4901-4914. Dio: 10.1029/2018wr024067

Pendergrass, A.G., 2018. What precipitation is extreme? Science 360 (6393), 1072 – 1073. Dio. 10.1126/science. aat1871

Steffen, W., Rockstrom, J., Richardson, K., Lenton, T.M., Folke, C., Liverman, D., Summerhayes, C.P., Barnosky, A.D., Cornell, S.E., Crufix, M., Donges, J.F., Fetzer, I., Lade, S.J., Scheffer, M., Winkelmann, R., Schellhuber, H.J., 2018. "Trajectories of the Earth System in the Anthropocene." *PNAS*, 115: 8252–59.

Seneviratne, S.I., Nicholls, N., Easterling, D., Goodess, C.M., Kanae, S., Kossin, J., Luo, Y., Marengo, J., McInnes, K., Rahimi, M., Reichstein, M., Sorteberg, A., Vera, C., Zhang, X (2012). Changes in climate extremes and their impacts on the natural physical environment. In: Managing the Risks of Extreme Events and Disasters to Advance Climate Change Adaptation. A Special Report of Working Groups I and II of the Intergovernmental Panel on Climate Change [Field CB, Barros V, Stocker TF, Qin D, Dokken DJ, Ebi KL, Mastrandrea MD, Mach KJ, Plattner G-K, Allen SK, Tignor M, Midgley PM (eds.)]. Cambridge University Press, Cambridge, UK and New York, NY, USA, pp. 109 -230.

Shongwe, M.E, Van Oldenborgh, G.J, Van den Hurk, B, Van Aalst M., 2011. Projected changes in mean and extreme precipitation in Africa under global warming. Part II: East Africa. J Climate 24: 3718–3733. http://doi.org/10.1175/2010JCLI2883.1.

Sillmann, J.V., Kharin, V., Zhang, X.W., Zwiers, F., Bronaugh, D., 2013b. Climate extremes indices in the CMIP5 multimodel ensemble: Part 2. Future climate projections. J. Geophys. Res., 118: 2473–2493. doi:10.1002/jgrd.50188.

Tan, G., Ayugi, B., Ngoma, H.N., Ongoma, V., 2020. Projections of Future Meteorological Drought Events under representative concentrations pathways (RCPs) of CMIP5 over Kenya, East Africa. *Atmosres*. https://doi.org/10.1016/j.atmosres.2020.105112

Tegegne, G., Melesse, A.M., Alamirew T., 2020. Projected changes in extreme precipitation indices from CORDEX simulations over Ethiopia, East Africa. Atmosres. https://doi.org/10.1016/j.atmosres.2020.105156

Taylor, K. E., Stouffer, R. J., Meehl, G.A., 2012. An overview of CMIP5 and the experiment design. Bull Am Meteorol Soc, *93*, 485-498. Dio. 10.1175/BAMS-D-11-00094.1

Ukkola, Anna M. et al. 2020. "Robust Future Changes in Meteorological Drought in CMIP6 Projections Despite Uncertainty in Precipitation." Geophys Res Lett 47: 1–9. Dio.10.1029/2020GL087820

Taylor, K.E., 2001. Summarizing multiple aspects of model perfomance in a Single Diagram. J. Geophys. Res, 106(D7), 7183–7192. https://doi.org/10.1029/2000JD900719.

Taylor, C.M. et al., 2017: Frequency of extreme Sahelian storms tripled since 1982 in satellite observations. Nature, 544, 475–478, doi:10.1038/nature22069

Trenberth, K. E., 2011: Changes in precipitation with climate change. Clim. Res. doi:10.3354/cr00953, in press.

Van Loon, A. F., Stahl, K., Di Baldassarre, G., Clark, J., Rangecroft, S., Wanders, N., Gleeson, T., Albert, I.J.M., Tallaksen, L.M., Hannaford, J., Uijlenhoet, R., Teulin, A., Hannah, D., Sheffield, J., Svoboda, M., Verbeiren, B., Wagener, T., Lanen, H.A.J., 2016. Drought in a human-modified world: reframing drought definitions, understanding, and analysis approaches. Hydrol.Earth Syst. Sci. 20, 3631-3650. doi:10.5194/hess-20-3631-2016

Viste, E., Korecha, D., Sorteberg, A., 2013. Recent drought and precipitation tendencies in Ethiopia. Theor and Appl. Climatol. 112, 535–551. https://doi.org/10.1007/s00704-012-0746-3.

Weber, T. Haensler, D, Rechid, Pfeifer, Eggert, B., Jacob, D., 2018: Analyzing regional climate change in Africa in a 1.5°C, 2°C and 3°C global warming world. Earth's Future, 6, 1–13, doi:10.1002/2017ef000714

Williams, A.P., Funk, C., 2011. A westward extension of the warm pool leads to a westward extension of the Walker circulation, drying eastern Africa. Clim. Dyn., 37, 2417–2435. https://doi:10.1007/s00382-010-0984-y

Wilks, S.D., 2006. Statistical methods in the Atmospheric Science. 2nd Edn. Academic Press

Yang, W., Seager, R., Cane, M.A., Lyon, B., 2014. The East African Long Rains in Observations and Models. J. Climate,27,7185–7202. https://doi.org/10.1175/JCLI-D-13-00447.1

Yuan, Z., Yang, Z., Yan, D., Yin, J., 2017. Historical changes and future projection of extreme precipitation in China. Theor Appl Climatol, 127, 393-407. Dio 10.1007/s00704-015-1643-3

Zhang, X., Alexander, L., Hegerl, G.C., Jones, P., Klein Tank, A., Peterson, T.C., Trewin, B., Zwiers, F.W., 2011. Indices for monitoring changes in extremes based on daily temperature and precipitation data. WIREs Clim. Chang. 2, 851–870. Dio. 10.1002/wcc.147

Zhu, H., Z. Jiang, J. Li, et al., 2020a: Does CMIP6 inspire more confidence in simulating climate extremes over China? *Adv. Atmos. Sci.*, doi: 10.1007/s00376-020-9289-1.